Nuclear Inst. and Methods in Physics Research, A 954 (2020) 161685

Contents lists available at ScienceDirect

Nuclear Inst. and Methods in Physics Research, A

journal homepage: www.elsevier.com/locate/nima

Development of a neutron spectrometer utilizing rubberized Eu:LiCAF wafers

Michael A. Ford [a,*], Buckley E. O'Day [a], John W. McClory [a], Areg Danagoulian [b]

[a] Air Force Institute of Technology, Department of Engineering Physics, 2950 Hobson Way, Wright-Patterson AFB, OH 45433, United States
[b] Massachusetts Institute of Technology, Department of Nuclear Science and Engineering, 77 Massachusetts Ave, Cambridge, MA 02139, United States

ARTICLE INFO

Keywords:
Neutron spectroscopy
Eu:LiCAF
Scintillator
WSF

ABSTRACT

A portable ten-layer neutron spectrometer has been developed using a novel material, LiCAF. The spectrometer consists of rubber matrix wafers with embedded europium doped lithium calcium aluminum fluoride (Eu:LiCAF) crystals and crosshatched wave shifting fibers (WSF). Layers of high density polyethylene (HDPE) separating each Eu:LiCAF wafer serve as neutron moderating material. Neutrons entering the spectrometer react in the Eu:LiCAF crystal, creating scintillation photons. The photons travel down the WSFs to silicon photomultipliers (SiPMs) that convert the photons to an electrical signal. Custom electronics are used to gather, amplify, process, and readout the signal. A library of several neutron response curves was created in Geant4 and MCNP. The experimental output of the spectrometer was unfolded using a maximum entropy algorithm, MAXED. The spectrometer was tested using two separate DD generators. These two tests resulted in unfolded neutron spectra with average neutron energies of 2.71 and 2.78 MeV and chi-squared values of 0.88 and 1.51 χ^2/D.O.F. respectively, when fit to a 2.45 MeV monoenergetic energy spectrum.

Contents

1. Introduction 1
2. LiCAF 2
3. Normalization 2
4. Experiment 3
5. Simulations 3
6. Results 4
7. Conclusions 6
Acknowledgments 7
References 7

1. Introduction

It has been a goal of the nuclear community to develop accurate, portable, and inexpensive neutron detection and spectroscopy techniques. The objective of this work was to incorporate novel Eu:LiCAF scintillators with custom electronics into a neutron spectrometer with the capability to measure the energy spectrum of neutrons in the domain of 1–10 MeV. This range of neutron energies was targeted specifically for identifying materials for nuclear security applications, however, the energy range can be easily adapted for different applications. Eu:LiCAF (europium doped lithium calcium aluminum fluoride) is the material of choice for this work because of its desirable properties: non-hygroscopic, low γ sensitivity, large size available, high scintillation light yield and transparency [1,2]. Eu:LiCAF offers significant advantages over using the current standard, ^{3}He, which is bulky and must be pressurized.

Ten wafers of rubberized Eu:LiCAF were obtained from Tokuyama Corporation, Japan to assemble a neutron spectrometer. The wafers were embedded with crosshatched wavelength shifting fibers (WSF) to absorb and convert the scintillation photons to a frequency that is compatible with SensL C-Series blue-sensitive silicon photo-multipliers (SiPMs). SiPMs were used to convert the scintillation photons into an electrical signal. Particle detector scintillation light has historically been collected with traditional photo-multiplier tubes, however, recent advances have greatly reduced the dark noise of SiPMs. Coupling the low dark noise with the great transparency and relatively high light-output

* Corresponding author.
E-mail address: michael.ford.15@us.af.mil (M.A. Ford).

https://doi.org/10.1016/j.nima.2018.11.144
Received 24 July 2018; Received in revised form 30 November 2018; Accepted 30 November 2018
Available online 14 January 2019
0168-9002/Published by Elsevier B.V.

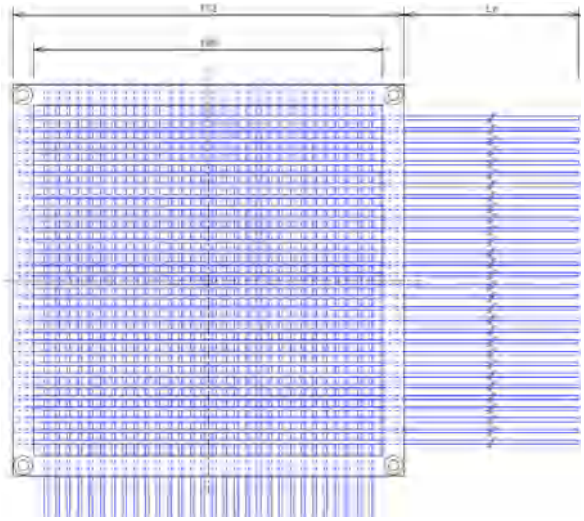

Fig. 1. CAD drawing of the LiCAF wafer from Tokuyama. (color online).

of Eu:LiCAF creates ideal conditions to introduce SiPMs to inelastic neutron scattering detectors [3–7].

Previous work with Eu:LiCAF indicates that it has the ability to perform well as a neutron detector [1,2,8]. Custom electronics were developed to readout, amplify, filter, and count Eu:LiCAF scintillation photons in a neutron flux [8]. A neutron spectrometer has been designed, fabricated, and tested in this work. The neutron counts are tallied for 10 layers, and the count data for each layer is unfolded to determine the energy spectrum of incident neutrons. The methodology of neutron counting with Eu:LiCAF, spectrometer construction, simulations, and neutron spectrum unfolding are discussed herein.

2. LiCAF

Eu:LiCAF/rubber (2×10^{21} ^{6}Li/cm^3), with an effective Z of 15 and density of 2.99 g/cm^3 was used throughout this work [9]. When compared to ^{3}He, the neutron absorption percentage of the rubber-matrix Eu:LiCAF is approximately 5% higher for 25 meV neutrons than it is for 10 atm ^{3}He [9]. A significant advantage of using Eu:LiCAF crystals in a rubber matrix is that the rubber suspends small Eu:LiCAF grains, which notably suppresses any signal generated by gamma interactions [2,8]. The interaction of interest in the Eu:LiCAF is the neutron absorption in ^{6}Li resulting in the reaction:

$$^{1}_{0}\mathrm{n} + ^{6}_{3}\mathrm{Li} \longrightarrow ^{3}_{1}\mathrm{H}\ (2.73\ \mathrm{MeV}) + ^{4}_{2}\mathrm{He}\ (2.05\ \mathrm{MeV}). \quad (1)$$

Due to their short range, the tritium and the alpha particles interact almost exclusively in the Eu:LiCAF crystal scintillator which creates scintillation photons that are transported via the WSFs to the SiPMs, where a current is created. The current is amplified and converted to a voltage signal, then filtered and converted to a digital signal using a comparator. The digital signals can then be counted/recorded using a field-programmable gate array (FPGA) or microcontroller. If data is collected from multiple layers of rubberized Eu:LiCAF, with varying amounts of neutron moderating material placed between the source and each Eu:LiCAF wafer, the resulting count data from the individual scintillators can be unfolded to determine the energy spectrum of incident neutrons.

The 10 cm × 10 cm × 0.5 cm wafers of rubberized Eu:LiCAF had 30 1 mm diameter wavelength shifting fibers embedded along both the X and Y axes to allow for position dependent readout, as shown in Fig. 1. Eu:LiCAF is known to have excellent transparency to its own light [9]. A light-tight box was placed around the entire wafer/electronics assembly to minimize ambient photon interactions with the SiPMs, which facilitates maintenance of a large signal-to-noise ratio. To further reduce the number of ambient photons, 3-D printed caps (black nylon, PA-11) were used to mount three adjacent parallel WSFs to each SiPM—for a total of 10 channels for each axis.

The electronics used to amplify the SiPM signal require a +/−5 V, ground, negative high voltage (approximately 30 V [10]), and a variable reference voltage for the comparator. The output of the electronics is a single wire for the digital pulse. The comparators are designed to output a digital "high" signal whenever the SiPM signal voltage exceeds a user-defined threshold.

Although the Eu:LiCAF has relatively low sensitivity to gammas, gamma interactions can occur and yield a detectable signal. However, due to the insensitivity of Eu:LiCAF crystals to photons, the primary source of gamma interactions is with the embedded WSFs. The scintillation pulses from the WSFs are much faster than those from the Eu:LiCAF. The gamma interactions in the WSFs and the Eu:LiCAF neutron interactions can thus be distinguished using a combination of pulse-shape analysis (filtering) and pulse-height discrimination [8]. The discrimination is possible because of the low-pass filter utilized in the circuit to suppress fast pulses, the low density of the rubberized Eu:LiCAF, the separation and small size of the Eu:LiCAF grains in the rubber matrix, and the fact that the neutrons deposit much more energy in the scintillator (from the high energy and short range of the alpha particle and triton). A combination of pulse shape filtering and pulse-height discrimination was used to count the neutrons that interacted in each layer of the spectrometer. This resulted in a clear distinction between the amplitude of neutron and gamma pulses, and provided confidence in the neutron counts recorded in each spectrometer layer as described in [8]. Simulations of the circuit were performed using LTSpice and the Eu:LiCAF counting methodology was validated in two independent experiments with two different DD generators [8].

3. Normalization

The neutron response of each Eu:LiCAF wafer was characterized prior to spectrometer construction. Normalization of each spectrometer layer was essential as a way to account for small differences in the wafers such as thickness, density, WSF placement, size of LiCAF grains, etc. An Adelphi Technology incorporated DD108 Neutron Generator at the Air Force Institute of Technology (AFIT) was used as a neutron source to normalize the wafers. The DD108 produces ~2.45 MeV neutrons at a continuous rate of 1×10^{9} n/s with 100 kV accelerating voltage, an operating beam current of 3 mA and deuterium flow rate of 8.0 SCCM. The samples were positioned perpendicular to the isotropic flow of neutrons at a distance of 20 cm where the neutron flux was approximately 2×10^{4} n/(cm^{2}s) during operation.

Each wafer was placed in the same configuration and location and subjected to the DD generator source for 5 min. A bias of negative 29.5 V was applied to each SiPM, and the wafers were enclosed in a 1.25 mm thick cadmium box to reduce the effect of thermal neutron inscatter from the test environment. Details of the calibration results are shown in Table 1, where the error in the correction factors is on the order of 0.0001%.

The neutron count rate for each layer was normalized to the least-performing wafer via the formula:

$$\text{Correction Factor}_i = \frac{L_{min}}{L_i} \quad (2)$$

where L_{min} is the total counts of the least-performing wafer, and L_i is the counts obtained by the ith wafer.

Upon calibration, the spectrometer was assembled and data was taken during 10 individual generator runs. Between each run, the same electronic circuit was moved to the next wafer. For example, the first run counted the neutrons in wafer #1, the next spectrometer run counted wafer #2, and run number 10 counted the neutrons in wafer #10. The next section discusses the experimental setup and results.

Table 1
Eu:LiCAF Wafer Normalization Parameters.

Wafer	Correction factor [#]	Neutron detection rate s^{-1} cm^{-2}
1	0.8659	19.4
2	0.9837	17.1
3	0.9448	17.8
4	1.0000	16.8
5	0.8622	19.5
6	0.9289	18.1
7	0.9553	17.6
8	0.9489	17.7
9	0.9367	18.0
10	0.8883	19.0

4. Experiment

The spectrometer was tested twice; first at AFIT, and the second time at the University of Michigan using a Thermo Scientific MP320 DD neutron generator with a rated flux of 1×10^6 n/s and a flux on the detector face of approximately 200 n/(cm^2s) [11]. Fig. 2 shows the spectrometer configuration. The data collection times were five minutes for runs at AFIT and for one hour at the University of Michigan. The run times were different between the two tests to account for the variance in neutron flux of the DD generators. The results of the experimental runs are shown in Figs. 3 and 4. Fig. 3 shows the neutron counts for each layer for the experiment conducted at AFIT, with a moderator thickness of 1.25 cm (HDPE). Fig. 4 shows the neutron counts for each layer for the experiment conducted at the University of Michigan, with a moderator thickness of 2.5 cm. The moderator thicknesses were chosen to account for the target energy range of the spectrometer (1–10 MeV); the 1.25 cm thickness was chosen for neutrons with energies near 1 MeV while neutrons with higher energies near 10 MeV require more moderation and therefore a thickness of 2.5 cm was tested. Geant4 simulations were used to optimize the moderator thickness used. The electronics were moved back one wafer for each successive generator run. While the Eu:LiCAF is segmented via embedded crosshatched fibers in both the X and Y axes, only the X-axis fibers were used for data collection. The fibers along the Y-axis were sealed with opaque tape. Both Figs. 3 and 4 show that there is an increase in counts toward the center of each layer. This is expected because of the increased neutron escape from scatters that occur toward the edges of the layers and was validated using Geant4 simulations. Total counts for each layer were obtained by summing each of the counts along the X-axis, then corrected using the normalization factors in Table 1.

The by-layer experimental results for the AFIT and University of Michigan testing are shown in Figs. 5 and 6, respectively. Fig. 5 shows that the experimental data very closely resembles the Geant4 simulation data. The neutron counts measured from each of the 10 layers was unfolded against simulation data to obtain the energy spectrum of the incident neutrons. Likewise, Fig. 6 shows the results of a 1-hour spectrometer run with a moderator thickness of 2.5 cm. While the data does closely resemble the simulations for the first 5 layers, layers 6–9 start to show deviation from the simulated response functions. The next section discusses the modeling, and potential reasons for the mismatch between experimental data and simulations.

5. Simulations

Simulations were used at several points in the spectrometer design, construction, and evaluation process. Simulations were used to determine the appropriate moderator thickness to resolve neutrons with energies of 1–10 MeV. Accurate simulations of the spectrometer and its surroundings were essential to allow unfolding and characterization of neutron energy spectra. Both MCNP6 and Geant4 simulations were conducted and yielded statistically indistinguishable results. Therefore,

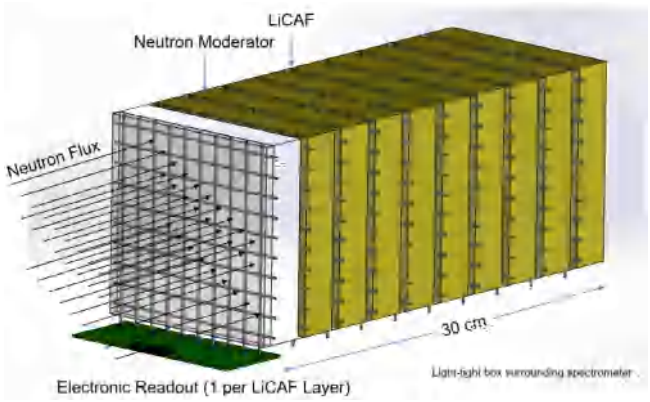

Fig. 2. Depiction of the ten-layer spectrometer assembly. Only one layer of electronics is shown. The entire assembly is enclosed in a light-tight box and wrapped in a 1.25 mm layer of cadmium. Detector wafers are 0.5 cm thick and the moderator thickness is either 1.25 or 2.50 cm, depending on the configuration. (color online).

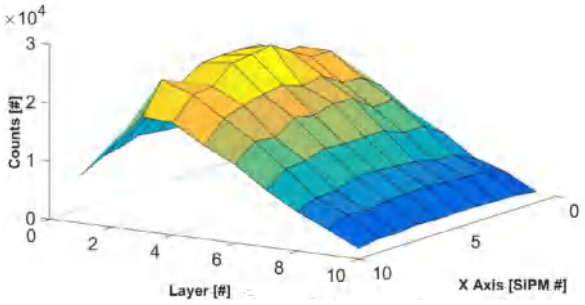

Fig. 3. 3-dimensional representation of spectrometer counts after five minute spectrometer run at AFIT's DD generator. Layer #1 is closest to the generator, and there are more counts toward the center of the spectrometer, as opposed to the boundaries. The HDPE moderator thickness for the spectrometer was 1.25 cm. (color online).

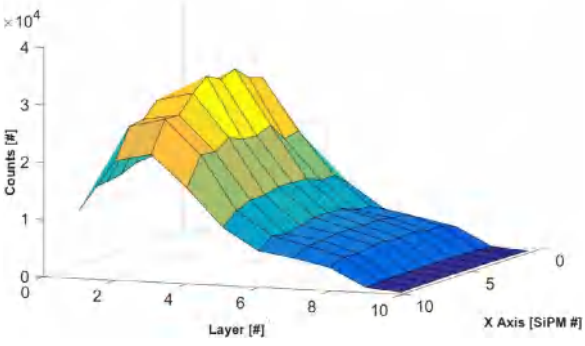

Fig. 4. 3-dimensional representation of spectrometer counts after 1-hour spectrometer run at University of Michigan's DD generator. Layer #1 is closest to the generator, and there are more counts toward the center of the spectrometer, as opposed to the boundaries. The HDPE moderator thickness for the spectrometer was 2.5 cm. (color online).

Geant4 simulations were used for unfolding. Simulations were run at both moderator thicknesses (1.25 and 2.5 cm), and the results were unfolded with MAXED using 23 energy bins. The response libraries are shown in Figs. 7 and 8 for the 1.25 cm and 2.5 cm moderator thicknesses, respectively. The response libraries are separated into two energy groups to better depict detector response behavior. The upper sections of Figs. 7 and 8 show energies from 0.001 MeV to 1.0 MeV and the bottom sections represent the range from 1.5 MeV to 10.0 MeV. The similarity of the response curves to adjacent energies seen in the larger energy range (above 3.5 MeV) complicates spectrum unfolding,

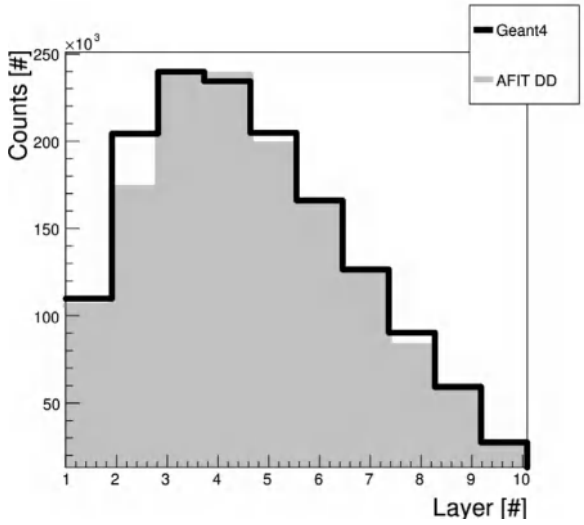

Fig. 5. Comparison between Geant4 simulation and data taken after five minute spectrometer run at AFIT's DD generator. Due to the small magnitude of the error bars, they are not represented in the plot.

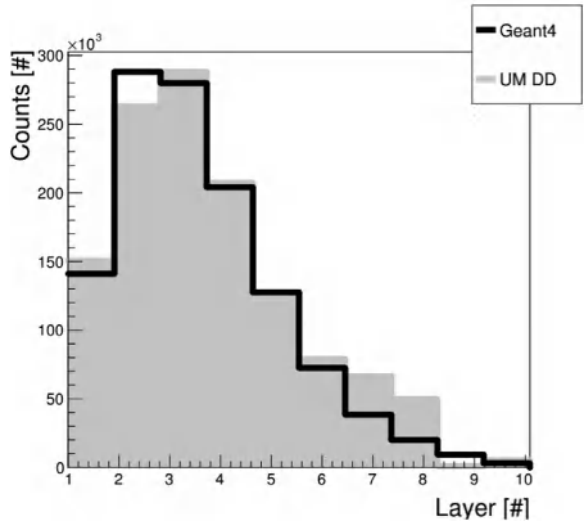

Fig. 6. Comparison between Geant4 simulation and data taken after 1-hour spectrometer run at University of Michigan's DD generator. Due to the small magnitude of the error bars, they are not represented in the plot.

requiring significantly more data to differentiate between adjacent energies.

Many efforts were made to reduce the effects of neutron scattering in the test environment. The spectrometer was surrounded by a layer of cadmium to minimize the slow neutrons from scattering into the spectrometer, and the walls around the DD generators were modeled to account for the higher energy neutrons that could potentially scatter around the room and back into the Eu:LiCAF wafers. There was a significant difference between count data and simulation results for the testing conducted at the University of Michigan. This is likely due to the crude modeling of the walls and the DD generator support table, without taking other factors into account, such as the DD generator housing, and other artifacts in the room. The higher neutron counts in the back layers of the spectrometer are indicative of back-scattering in the environment of higher energy neutrons that enter from the rear of the spectrometer and subsequently moderated and absorbed. Because of the increased experimental counts at more-forward layers in the spectrometer testing at the University of Michigan, and because of the

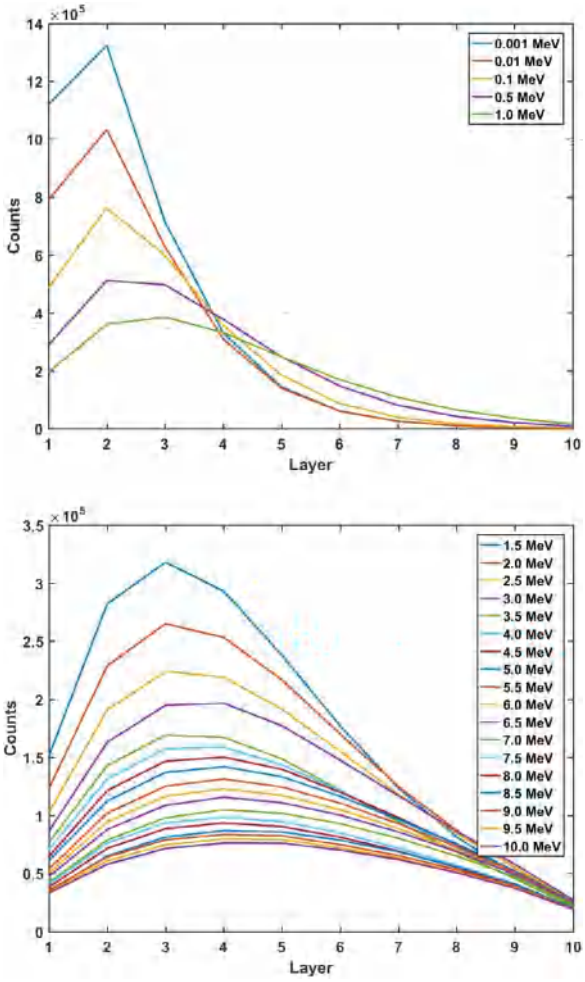

Fig. 7. Response libraries created in Geant4 to model the spectrometer response for energies from 0.001 MeV to 10.0 MeV with a moderator thickness of 1.25 cm and the walls/DD generator support table at the Air Force Institute of Technology. (color online).

close-overlap of response curves for layers 6–10 (Fig. 8 (bottom)), it was expected that there would be large errors evident in unfolding the neutron energy spectrum.

6. Results

Unfolding a spectrum with only a few channels of data is not a trivial problem, as there is no unique solution and the response functions are generally smooth and overlap over many orders of magnitude. The Maximum Entropy Deconvolution code (MAXED) was used here for unfolding. MAXED [12,13] is an algorithm developed to apply the maximum entropy principle to the problem of unfolding neutron spectroscopic measurements. Using only 10 data points from the spectrometer, the neutron spectrum is unfolded in discrete energy groups (n energy bins with index i, and m layers with index k). The solution is not unique, however the set of admissible spectra is defined using two restrictions [13]:

$$N_k + \epsilon_k = \sum_i R_{ki} f_i \tag{3}$$

$$\sum_k \frac{\epsilon_k^2}{\sigma_k^2} = \Omega \tag{4}$$

where N_k is the experimentally obtained value for layer k, ϵ_k is the difference between the predicted value and the measured value for layer k, R_{ki} is the response function for layer k, f_i is the solution spectrum

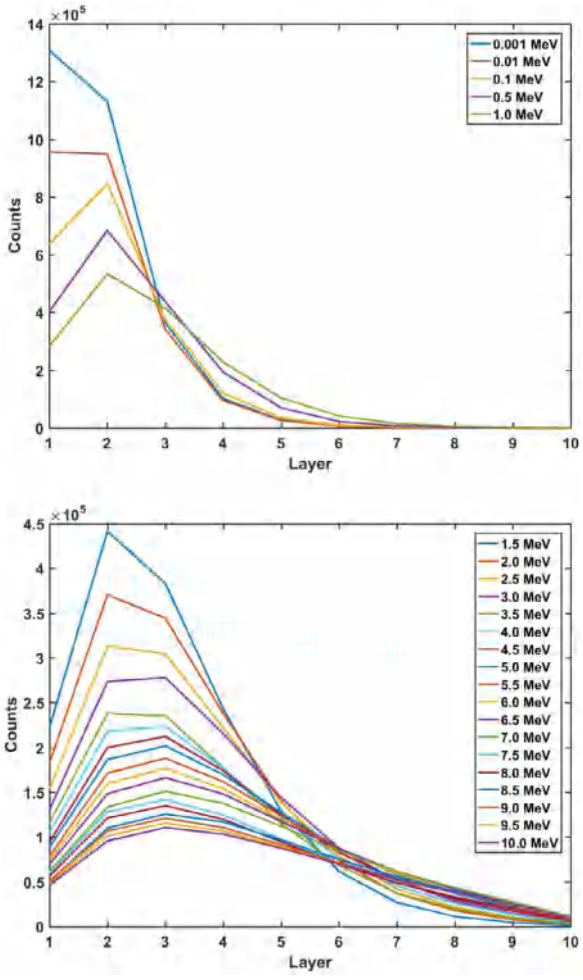

Fig. 8. Response libraries created in Geant4 to model the spectrometer response for energies from 0.001 MeV to 10.0 MeV with a moderator thickness of 2.50 cm and the walls/DD generator support structure at the University of Michigan. (color online).

with i discrete energy groups, σ_k is the estimated standard uncertainty ($\sqrt{N_k}$ in this case), and Ω is a parameter set by the user defining how well to try to fit the solution spectrum to the a priori data. MAXED uses a simulated annealing algorithm to maximize the entropy (S) of the solution spectrum [14]:

$$S = -\sum\left(f_i \ln\left(\frac{f_i}{f_i^{DEF}}\right) + f_i^{DEF} - f_i\right) \tag{5}$$

where f_i^{DEF} is the default spectrum that contains the a priori information (for this work, the a priori spectrum was defined as a peak of 2.45 MeV neutrons). When analyzing data from multi-layer spectrometers, the a priori information includes estimates of the neutron source, as well as information about the physics governing neutron interactions as they travel from the source to the spectrometer [13].

The simulated annealing algorithm maximizes the entropy of the unfold Eq. (5). The algorithm can be considered analogous to the physical process by which a material changes state while minimizing its energy [15]. A slow, careful cooling often results in a highly ordered crystalline state of lowest energy while a rapid cooling instead yields defects inside the material [16]. The temperature reduction factor (TRF) is applicable in cases where a parameter maximization function is very likely to become stationary in a metastable, local minimum. Simulated annealing permits uphill moves under the control of a temperature parameter, the TRF. The TRF allows the user to adjust the "step size" applied in the simulated annealing algorithm. At higher temperature,

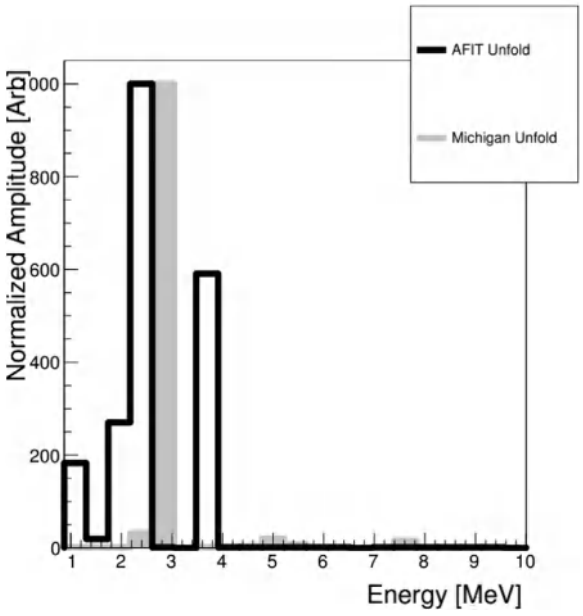

Fig. 9. MAXED deconvolution of spectrometer run at both AFIT and University of Michigan with temperature reduction factor of 0.85 and an a priori spectrum of monoenergetic 2.45 MeV neutrons.

Table 2
DD Generator Unfolding Results.

Temp. Red. Factor	AFIT		MI	
	μ(Energy)	χ^2/D.O.F	μ(Energy)	χ^2/D.O.F
.90	2.71	0.88	3.67	30.09
.85	2.66	1.58	3.15	79.79
.80	2.71	1.10	3.03	641.6
.75	2.77	1.38	3.03	47.61
.70	2.62	1.77	3.04	31.69
.65	2.75	1.19	3.82	41.14
.60	2.82	1.12	2.96	31.38
.55	2.77	1.18	2.97	93.90
.50	2.70	1.91	3.06	89.77
.45	2.80	1.42	3.17	34.74
.40	2.80	1.56	3.04	32.18
.35	2.77	1.06	5.54	186.5
.30	2.72	1.12	2.96	38.03

only the gross behavior of the maximum entropy function is relevant to the search for the global minimum. As temperature decreases, however, finer details can be developed to locate the maximum entropy. Several temperature reduction factors were evaluated to determine how they affect the resulting unfold. The results of the temperature analysis are shown in Table 2.

The requested χ^2/D.O.F. was held constant at 1.0 through all of the unfolds and the only parameter that was varied was the TRF. The χ^2/D.O.F. was calculated in each step of the MAXED algorithm and compares the a priori spectrum to the MAXED output. Although the requested χ^2/D.O.F. was 1.0 for each MAXED unfold, this value was not always attainable. Because of the problem with uniqueness, using a priori data allows a "starting point", and then the entropy is maximized from that point in order to determine a final spectrum that accounts for new information and the a priori data [13]. A formal argument used in information theory shows that for this type of spectrum unfolding, the maximum entropy method is the *only* known general method of solving this problem that does not lead to inconsistencies [13].

The recommended TRF for MAXED unfolding is 0.85 [12], and these unfolding results are shown in Fig. 9. The average energy, μ(Energy), of the spectrum was calculated for the unfold results since the a priori spectrum consisted only of monoenergetic 2.45 MeV neutrons. Via

Table 3
Unfold errors and final λ values for AFIT.

#	C/M Ratio	StDev(C/M) from Total Unc.	StDev(C/M) from Stat Unc.	Lambda (λ)
1	1.07786	0.1539	0.00452	8.325691E−4
2	1.05663	0.1496	0.00350	2.526442E−4
3	1.02920	0.1463	0.00293	−1.977880E−4
4	0.99848	0.1441	0.00290	−4.266265E−4
5	1.03150	0.1471	0.00323	3.820434E−6
6	0.99477	0.1454	0.00349	−4.348146E−4
7	0.98025	0.1454	0.00398	−7.553486E−4
8	1.03699	0.1526	0.00501	9.772045E−4
9	0.97084	0.1512	0.00583	−1.214619E−3
10	1.06661	0.1744	0.00944	5.422050E−3

Table 4
Unfold errors and final λ values for Michigan.

#	C/M Ratio	StDev(C/M) from Total Unc.	StDev(C/M) from Stat Unc.	Lambda (λ)
1	0.79775	0.01322	0.00330	−8.837561E−5
2	0.95649	0.01409	0.00270	1.447682E−4
3	0.88382	0.01358	0.00249	3.320812E−5
4	0.94775	0.01411	0.00303	8.425696E−5
5	1.02039	0.01484	0.00399	2.320704E−4
6	1.00078	0.01504	0.00504	2.232096E−4
7	0.68469	0.01301	0.00470	−1.903631E−3
8	0.50573	0.01229	0.00502	−1.159838E−2
9	1.14281	0.02084	0.01429	1.771052E−2
10	0.84415	0.01321	0.01791	4.437544E−3

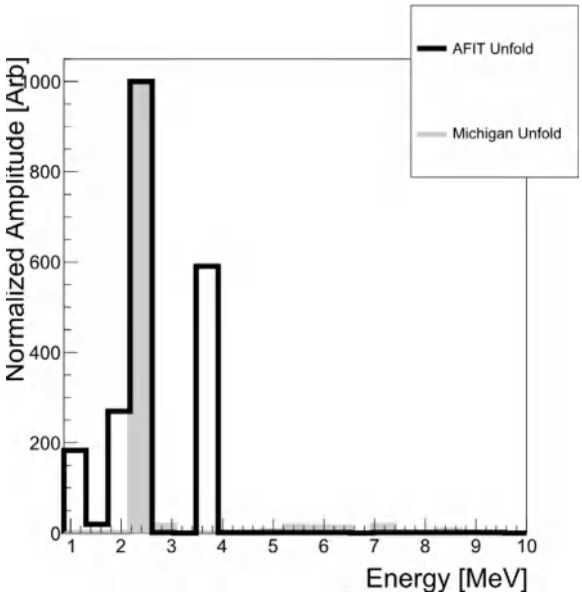

Fig. 10. Results of MAXED run at a temperature reduction factor of 0.85 for the first five layers of University of Michigan spectrometer data, versus the full 10 layer unfold of AFIT data. The incident neutron energy is deconvoluted with an a priori spectrum of monoenergetic 2.45 MeV neutrons.

the χ^2 goodness-of-fit test, if χ^2/D.O.F$\approx$ 1.0, then the MAXED unfold is in satisfactory agreement with the default spectrum. Likewise, if χ^2/D.O.F$\gg$ 1.0, then the fit is not satisfactory. Using the recommended TRF value, the second row of Table 2 shows that an average energy of 2.66 MeV was determined with a χ^2/D.O.F of 1.58 for the spectrometer test at AFIT, and an average energy of 3.15 MeV was obtained with a χ^2/D.O.F of 79.79 for the testing at University of Michigan. The higher counts in layers 6–9 of the spectrometer test at Michigan resulted in a higher net energy and poor result for the unfolding χ^2 metric. The AFIT spectrometer test, however, shows a good distribution near 2.45 MeV, and all of the χ^2 values obtained are within one standard deviation of 1.0 on the chi-squared distribution plot. While there is no error reported for the final average energy obtained using MAXED, Tables 3 and 4 show the calculated/measured (C/M) ratio for each of the 10 Eu:LiCAF detectors, and also the computed λ_k values for each of the wafers. MAXED outputs the C/M ratio and the StDev(C/M) using the measured counts input by the user, their respective errors, and the MAXED calculated counts after maximizing the entropy in the deconvolution. The simulated annealing algorithm produces values for λ_k which are related to the final energy spectrum via [17]:

$$f_i = f_i^{DEF} exp\left(-\sum_k \lambda_k R_{ki}\right) \tag{6}$$

Any change of the input parameters (N_k, σ_k, f_i^{DEF}, R_{ki}, and Ω) will lead to a change in the output parameters λ_k (shown in the last column of Tables 3 and 4). The error of the resultant energy spectrum is difficult to quantify because of the correlated errors between the experimentally obtained counts of each layer, and also the errors in the default spectrum used for unfolding. MAXED does propagate errors, and the net standard deviation for the calculated/measured ratios are reported in the third and fourth columns of Tables 3 and 4. These are the uncertainties calculated with the assumption that the correlated errors are defined by a matrix B:

$$B = \begin{pmatrix} \sigma_1^2 & & & \\ & \sigma_2^2 & & \\ & & \ddots & \\ & & & \sigma_m^2 \end{pmatrix}$$

For changes in the measured data, the uncertainty matrix is defined by [17]:

$$U = \frac{\delta f}{\delta N} \cdot B \cdot \left(\frac{\delta f}{\delta N}\right)^T . \tag{7}$$

Propagated error for the default spectrum is calculated in a similar way. However, since this error does not translate into the resultant energy spectrum, an effort was made to define the uncertainty in the unfold by considering the spread of data as a result of varying the temperature reduction factor. This results in a value for the AFIT tests of 2.7390 ± 0.0315 MeV and a value for the University of Michigan testing of 3.3412 ± 0.3886 MeV.

This research shows that by using Eu:LiCAF, and portable, custom electronics, a simple spectrometer has the ability to accurately identify the energy of mono-energetic neutrons if the a priori information is accurate. It was also shown here that the unfolded energy spectrum is extremely sensitive to proper modeling of the testing environment. The geometry of the testing area at AFIT was arguably more simple, as the entire spectrometer area was surrounded by concrete. There were many pieces of auxiliary equipment in the University of Michigan testing area that were not accounted for in the simulations, likely causing the large mismatch between the simulations and experimental results.

In an effort to improve the results of the University of Michigan spectrometer tests, the data was unfolded for a second time using only the first five layers of data. Since the hypothesized backscatter is primarily evident in the last half of the spectrometer, utilizing only the first five layers was explored to reduce the effect of the scattering, and to produce a better fit to the 2.45 MeV neutrons. The results of the five-layer unfold are shown in Fig. 10. Performing the unfold with a reduced number of layers improved the fit of the Michigan data to an energy of 2.78 MeV with a χ^2/D.O.F. of 1.51. A disadvantage of the five-layer unfolding, compared to the 10 layers (although not quantified herein) is an increase in uncertainty. The reduced-layer unfold demonstrated that the spectrometer is capable of identifying the energy of a mono-energetic neutron source even in the presence of anomalies in the data.

7. Conclusions

A portable neutron spectrometer has been developed using alternating layers of Eu:LiCAF and HDPE. Portability of the spectrometer

was maintained by utilizing custom electronics requiring only ±5 V, a negative bias voltage supply of approximately 30 V, and a variable voltage supply for setting the user-defined threshold level. Eu:LiCAF is able to differentiate gammas from neutrons using pulse-height discrimination in conjunction with pulse shape filtering, and ambient photons and thermal neutrons are shielded with a light-tight box and a layer of cadmium, respectively. MAXED was used to unfold the spectrometer data into a neutron energy spectrum, and the commissioning run at the Air Force Institute of Technology yielded an average neutron energy of 2.71 MeV with a χ^2 value of 0.88/D.O.F. when fit to a monoenergetic neutron energy spectrum of 2.45 MeV.

A primary goal of this work was to research a mechanism for identifying a neutron signature in the range of 1–10 MeV. Future work will focus on characterizing the spectrometer response at energies closer to 10 MeV and also with polyenergetic spectra. This future work will require a concentration on optimizing the HDPE layer thickness (potentially using non-uniform layer thicknesses), and also simulations that are tailored to the specific testing scenarios. Future testing will also be conducted to determine how well the Eu:LiCAF wafers discriminate higher energy gammas.

Acknowledgments

This work was supported at the Air Force Institute of Technology by the Defense Threat Reduction Agency, USA (HDTRA17-245-26). Views expressed in this paper are those of the authors and do not necessarily reflect the official policy or position of the Air Force, the Department of Defense, or the United States Government.

References

[1] M. Woodring, R. Kouzes, M. Demboski, R. Cameron, J. Magana, Characterization of the Tokuyama Corporation LiCAF Neutron Detector, Tech. Rep., Pacific Northwest National Laboratory, 2015, http://dx.doi.org/PNNL-ACT-10032.

[2] L. Viererbl, V. Klupák, M. Vinš, M. Koleška, J. Šoltés, A. Yoshikawa, M. Nikl, LiCaAlF 6 scintillators in neutron and gamma radiation fields, Int. J. Modern Phys. Conf. Ser. 44 (2016) 1660234, http://dx.doi.org/10.1142/S2010194516602349.

[3] M. Foster, D. Ramsden, A compact neutron detector based on the use of a SiPM detector, in: IEEE Nuclear Science Symposium Conference Record, 2008, pp. 1882–1886, http://dx.doi.org/10.1109/NSSMIC.2008.4774758.

[4] J.B. Mosset, A. Stoykov, U. Greuter, M. Hildebrandt, N. Schlumpf, H. Van Swygenhoven, Evaluation of two thermal neutron detection units consisting of ZnS/ 6LiF scintillating layers with embedded WLS fibers read out with a SiPM, Nucl. Instrum. Methods Phys. Res. A 764 (2014) http://dx.doi.org/10.1016/j.nima.2014.07.060.

[5] A. Stoykov, J.B. Mosset, U. Greuter, M. Hildebrandt, N. Schlumpf, A SiPM-based ZnS:^{6}LiF scintillation neutron detector, 2015, http://dx.doi.org/10.1016/j.nima.2015.01.076, arXiv:1408.6119.

[6] S. Gnecchi, C. Jackson, A 1 × 16 SiPM array for automotive 3d imaging LiDAR systems, Int. Image Sensor Soc. (2017) 133–136.

[7] N. Rhodes, Scintillation detectors, Neutron News (23) (2012) 26.

[8] M.A. Ford, B.E. O'Day, J.W. Mcclory, S.K. Manish, A. Danagoulian, Evaluation of Eu:LiCAF for neutron spectroscopy utilizing SiPMs and portable electronics, Nucl. Instrum. Methods Phys. Res. A (2018) http://dx.doi.org/10.1016/j.nima.2018.08.106.

[9] K. Fukuda, Scintillators Developed by Tokuyama for Neutron Detection Functional Fluoride Group, Tech. Rep., Tokuyama Corporation, 2014.

[10] SensL, C-Series Low Noise Fast Blue-Sensitive Silicon Photomultipliers, Tech. Rep., SensL Corporation, 2014.

[11] Thermo Scientific, Thermo Scientific MP 320 Lightweight, Portable Neutron Generator Thermo Scientific MP 320 Neutron Generator, URL https://assets.thermofisher.com/TFS-Assets/CAD/Specification-Sheets/D10497{-}.pdf.

[12] M. Reginatto, P. Goldhagen, MAXED, A Computer Code For the Deconvolution of Multisphere Neutron Spectrometer Data Using The Maximum Entropy Method, Tech. Rep., US Department of Energy, 1998.

[13] M. Reginatto, P. Goldhagen, S. Neumann, Spectrum unfolding sensitivity analysis and propagation of uncertainties with the maximum entropy deconvolution code MAXED, Nuclear Instrum. Methods Phys. Res. A 476 (1–2) (2002) 242–246, http://dx.doi.org/10.1016/S0168-9002(01)01439-5.

[14] J. Skilling, Maximum Entropy and Bayesian Methods, Cambridge, England, 1988.

[15] W.L. Goffe, G.D. Ferrier, J. Rogers, Global optimization of statistical functions with simulated annealing, J. Econometrics 60 (1–2) (1994) 65–99, http://dx.doi.org/10.1016/0304-4076(94)90038-8.

[16] A. Corana, M.C. Martini, S. Ridella, Corrigenda: Minimizing multimodal functions of continuous variables with the 'simulated annealing' algorithm, ACM Trans. Math. Software 15 (3) (1989) 287, http://dx.doi.org/10.1145/66888.356281.

[17] ORNL, RSICC Peripheral Science Routine Collection - Monteburns 2.0 - Psr-455, Tech. Rep., Oak Ridge National Laboratory, 2003.